Materials Letters 65 (2011) 579–582

Contents lists available at ScienceDirect

Materials Letters

journal homepage: www.elsevier.com/locate/matlet

Synthesis, characterization and magnetic properties of hexagonal $(VO)_{0.09}V_{0.18}Mo_{0.82}O_3 \cdot 0.54H_2O$ microrods

G.S. Zakharova [a,*], V.L. Volkov [a], C. Täschner [b], I. Hellmann [b], R. Klingeler [b], A. Leonhardt [b], B. Büchner [b]

[a] Institute of Solid State Chemistry, Ural Division, Russian Academy of Sciences, Pervomaiskaya ul. 91, Yekaterinburg, 620990, Russia
[b] Leibniz-Institut für Festkörper- und Werkstoffforschung IFW Dresden, Helmholtzstr. 20, D-01069 Dresden, Germany

ARTICLE INFO

Article history:
Received 15 September 2010
Accepted 2 November 2010
Available online 6 November 2010

Keywords:
Molybdenum oxides
Vanadium oxide
Rods
Hydrothermal synthesis
Metastable phase
Hexagonal structure
Magnetic properties

ABSTRACT

$(VO)_{0.09}V_{0.18}Mo_{0.82}O_3 \cdot 0.54H_2O$ microrods have been synthesized for the first time via a hydrothermal treatment of aqueous peroxomolybdic acid and vanadyl sulfate. The compound crystallizes in hexagonal rods with space group $P6_3$, and lattice constants $a = 10.586$ Å, and $c = 3.698$ Å. The single crystalline rods exhibit diameters of 1–2 μm and lengths up to 45 μm. A variety of techniques, including X-ray diffraction, scanning electron microscopy, high-resolution transmission electron microscope, Fourier-transform infrared spectroscopy, differential scanning calorimetry and static magnetometry were used to characterize the product.

1. Introduction

Molybdenum compounds have received considerable attention because of their applicability in catalytic and electrochemical processes. Molybdenum trioxide exists in several polymorphic forms, e.g., stable α-MoO_3 as well as metastable β- and hexagonal *h*-phases [1–3]. Metastable structures can demonstrate novel and unusual properties as compared to their thermodynamically stable phases [4]. A series of vanadium-stabilized hexagonal MoO_3 compounds with the general formula $M_xV_xMo_{1-x}O_3 \cdot nH_2O$ (M = Li, Na, K, Rb, Cs, and NH_4) has been prepared by a soft chemistry method [5–9]. The structure of these materials exhibits zigzag chains of edge-coupled octahedra which leads to the formation of one-dimensional channels parallel to the *c*-axis [10]. Monovalent cations occupy the large tunnel sites stabilizing the hexagonal structure. Dupont L. et al. [8,11] studied phase transformations between metastable hexagonal and stable orthorhombic MoO_3 structures in $H_xV_xMo_{1-x}O_3 \cdot 0.3H_2O$ ($0.06 \le x \le 0.18$) compounds.

In this paper, we report about hydrothermally synthesized hexagonal $(VO)_{0.09}V_{0.18}Mo_{0.82}O_3 \cdot 0.54H_2O$ rods stabilized by $(VO)^{2+}$ divalent cations in the channels. The material has been characterized by a combination of SEM, TEM, XRD, and thermal analysis methods as well as magnetic measurements.

2. Experimental

The starting chemicals were reagent grade molybdenum powder (99.9% metal), reagent grade 30% hydrogen peroxide, and vanadyl sulfate $VOSO_4 \cdot nH_2O$ (19.9% V) from Sigma-Aldrich. A typical synthesis procedure was carried out as follows: 0.5 g of molybdenum powder was dissolved in 10 ml hydrogen peroxide at 5–10 °C. The peroxide solution was subsequently mixed with an aqueous solution containing 0.56 g vanadyl sulfate hydrate (molar ratio $Mo^{6+}:V^{4+} = 1:0.5$) under stirring to homogeneity for 1 h. The mixture was transferred into a stainless steel autoclave with PTFE cup (23 ml capacity) and then constantly kept at 160 °C for 5 days. After being air-cooled to room temperature the precipitate was collected, washed with water, and vacuum-dried at 60 °C. The molybdenum and vanadium contents were determined using mass spectroscopy (Spectromass 2000). The vanadium(IV) concentration was obtained by volume titration with $KMnO_4$. The phase analysis was performed by X-ray diffraction (DRON-2, Cu Kα radiation, $\lambda = 1.5418$ Å). The final refinement of the structural parameters was done by a full-profile analysis using the FULLPROF-2006 software. The morphology of the powders was determined on a FEI Tecnai F30 high-resolution transmission electron microscope (HRTEM) and a Nano-SEM (FEI) scanning electron microscope (SEM). Fourier-transform infrared spectra were recorded on a Perkin-Elmer Fourier-transform spectrometer with a resolution of 0.5 cm^{-1}. Differential scanning calorimetry (DSC) was carried out using a DTA 409 PC/PG thermoanalyzer (Netzsch). Magnetization measurements have been performed using a SQUID magnetometer (Quantum Design MPMS XL5). The applied field was

* Corresponding author.
E-mail address: volkov@ihim.uran.ru (G.S. Zakharova).

0167-577X/$ – see front matter © 2010 Elsevier B.V. All rights reserved.
doi:10.1016/j.matlet.2010.11.001

$\mu_0 H = 1$ Tesla and the data were obtained in the temperature range from 2 to 320 K.

3. Result and discussion

Fig. 1 shows the X-ray diffraction analysis of the resulting product. All diffraction peaks can be indexed within the space group $P6_3/m$. The X-ray pattern looks like that of hexagonal MoO_3 (JCPDS 21-0569). The lattice parameters are $a = 10.586$ Å, $c = 3.698$ Å, and $V = 358.87$ Å^3. The Bragg R-factor equals 1.84, the R_f-factor = 2.96. No peaks of any other phase are detected which indicates the purity of the final product. The VO^{2+} implantation into the structure results in the increase of the a parameter compared to the hexagonal MoO_3 phase while the c parameter is rather unaffected. Similar data about the cation introducing influence on the a and c parameters were reported earlier [7]. This behavior can be explained by the fact that cations in the tunnels have neighbors along the a- and b-axis, but not along the c-axis. Note, that the strong diffraction peaks corresponding to (h00) reflections imply an oriented anisotropic growth of the rods in the [001] direction.

The size and shape of the resulting crystals were examined by SEM and HRTEM (Figs. 2 and 3). Our data do not exhibit any indication of an impurity phase, i.e. within the error bars of the SEM, EDX, and XRD data the rods are phase pure. The as-prepared material shows a unique rod-like morphology, with a hexagonal cross section of these rods. The diameter of the rods amounts to 1–2 μm and the length is up to 45 μm (Fig. 2). The HRTEM image of an individual rod (Fig. 3) shows that it is constituted with layered structure plates. The lattice fringes correspond to a d-spacing of 0.92 nm which is in good agreement with the d_{100}-spacing value from the XRD patterns of the hexagonal phase. The edges of the rods are smooth. In summary, all results demonstrate that individual rods with high crystallinity have been produced. The EDX analysis (Fig. 2c) only finds the elements Mo, V and O but no traces of any impurities in the final product. According to the analytical data, the general formula of the new vanadyl-stabilized hexagonal MoO_3 phase is $(VO)_{0.09}V_{0.18}Mo_{0.82}O_3 \cdot 0.54H_2O$.

Fig. 3a depicts the FTIR spectrum of the $(VO)_{0.09}V_{0.18}Mo_{0.82}O_3 \cdot 0.54H_2O$ sample. The FTIR spectra show three peaks at 555, 921, 980 cm^{-1}, and one shoulder at 715 cm^{-1}, respectively. The sharp bands at 980 and 921 cm^{-1} are attributed to the stretching vibration of the Mo=O double bond. This signal was also found in the orthorhombic MoO_3 phase pointing to the terminal oxygen bonds in the framework [12]. The

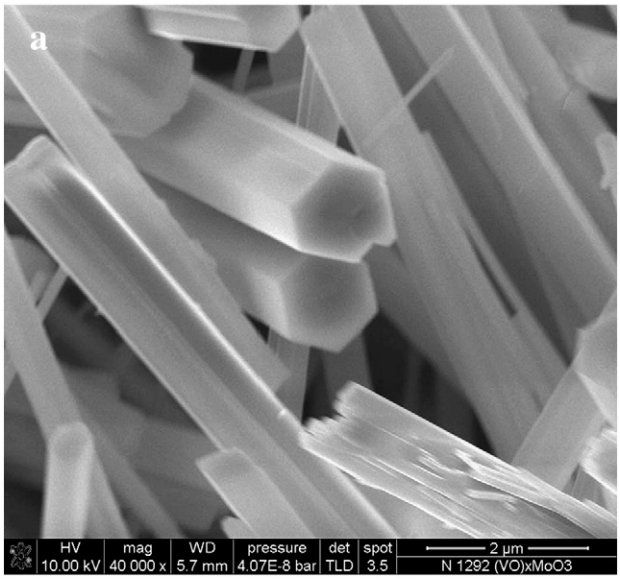

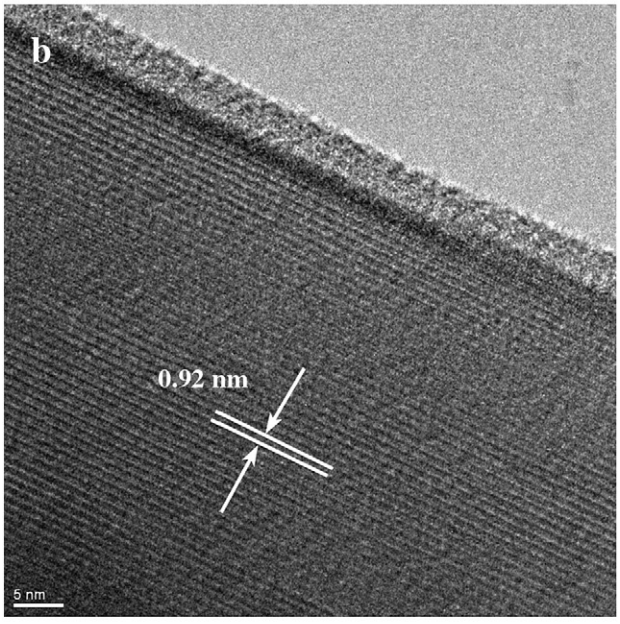

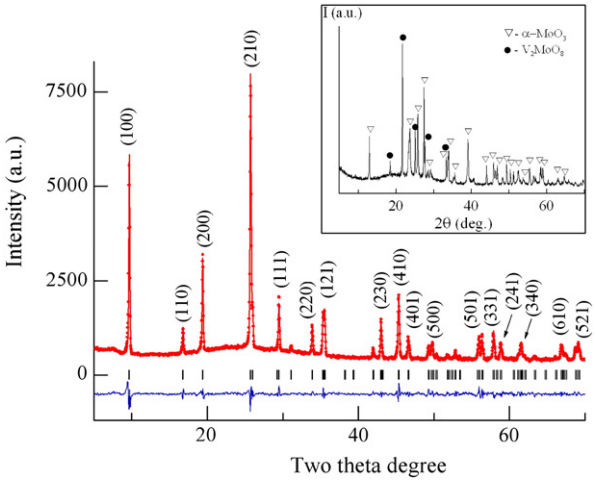

Fig. 1. Experimental (solid line), calculated (circles) and difference (bottom) plot for $(VO)_{0.09}V_{0.18}Mo_{0.82}O_3 \cdot 0.54H_2O$ rods. Vertical lines show reflection positions (Cu-Kα_1 and Cu-Kα_2 radiation). The inset shows XRD diffractogram of the sample after annealing at 500 °C.

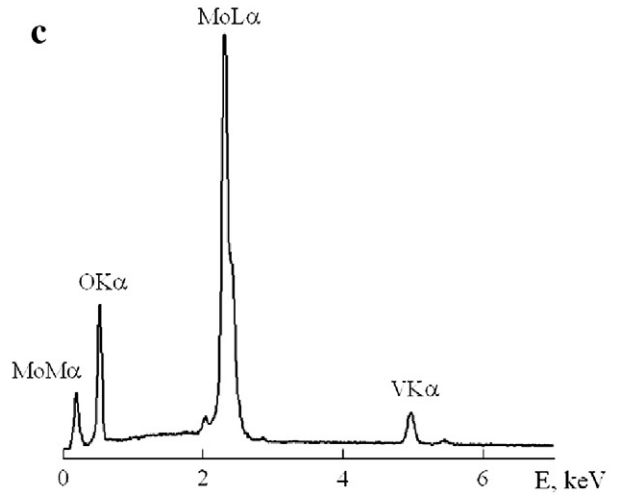

Fig. 2. (a) Typical SEM and (b) TEM images, and (c) EDX pattern for $(VO)_{0.09}V_{0.18}Mo_{0.82}O_3 \cdot 0.54H_2O$ rods.

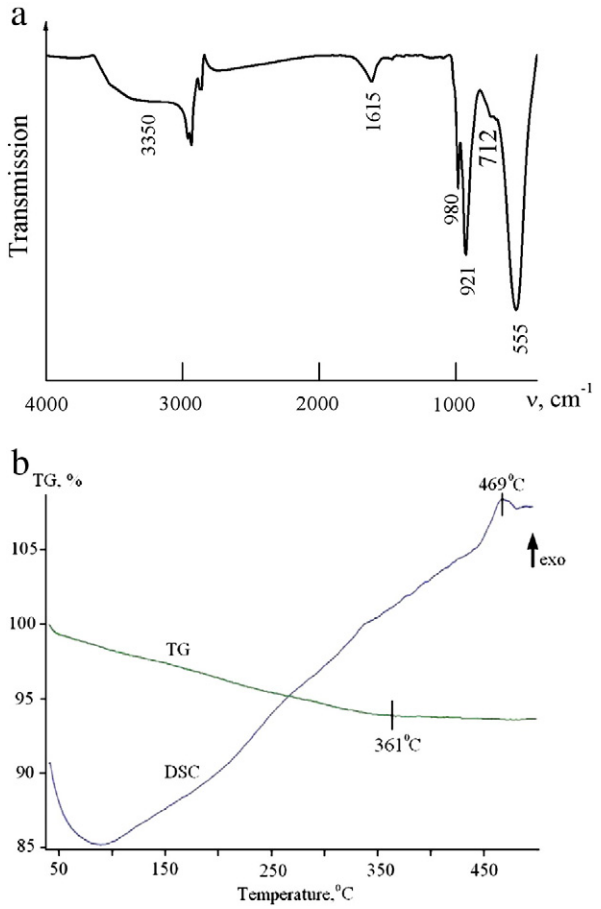

Fig. 3. (a) IR spectrum, (b) DSC and TG scans of $(VO)_{0.09}V_{0.18}Mo_{0.82}O_3 \cdot nH_2O$ rod powders (8.6 mg).

signals at 712 and 555 cm^{-1} are related to stretching and bending vibrations with different Mo–O bond lengths [13,14]. The broad band at 3350 cm^{-1} is assigned to –OH stretching vibrations from water. The $\delta(H_2O)$ deformation vibrations give an asymmetric band centered at 1615 cm^{-1}. This band is ascribed to the adsorbed water in the sample.

Data of the thermal and gravimetric analysis (DSC and TG) of the $(VO)_{0.09}V_{0.18}Mo_{0.82}O_3 \cdot 0.54H_2O$ sample are shown in Fig. 3b. According to the TG curve, the integrated loss is as high as 6.4%; the weight of the sample decreases continuously up to 361 °C. The broad endothermic effect visible in the DSC data demonstrates the dehydration process during heating. According to the XRD data product of the dehydration the *h*-MoO_3 structure is retained. Then the DSC signal exhibits a strong exothermic peak at 469 °C. This exothermic effect associated with a phase transition of the MoO_3 polymorphs [6–8,11]. Examination of the final product by XRD showed that the annealing induces the bulk decomposition. During annealing the hexagonal metastable $(VO)_{0.09}V_{0.18}Mo_{0.82}O_3 \cdot 0.54H_2O$ compound transforms into the thermodynamically stable orthorhombic modification of the α-MoO_3 phase and the complex oxide V_2MoO_8 (see the inset in Fig. 1). According to XRD data this process is proved to be irreversible. The decomposition temperature of the $(VO)_{0.09}V_{0.18}Mo_{0.82}O_3 \cdot 0.54H_2O$ rods indicates that the vanadyl ions have a stabilizing effect in comparison with metallic cations or ammonium in the hexagonal tunnels of MoO_3 [6–8].

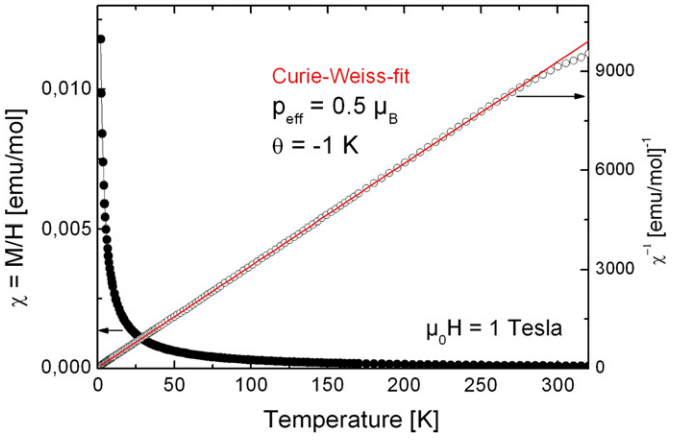

Fig. 4. Static susceptibility $\chi = M/H$ of the $(VO)_{0.09}V_{0.18}Mo_{0.82}O_3 \cdot 0.54H_2O$ rods vs. temperature in an external magnetic field of $\mu_0 H = 1\ T$ (circles). The solid line indicates the Curie–Weiss law which has been fitted to the data (see the text).

Measurements of the static magnetic susceptibility $\chi = M/B$ vs. temperature are displayed in Fig. 4. According to the linear temperature dependence of the inverse susceptibility $\chi^{-1}(T)$, the sample exhibits paramagnetic behavior in the whole temperature range. The data can be described in terms of the Curie–Weiss law $\chi(T) = C/(T+\theta)$, with the Curie–Weiss temperature θ and the Curie-constant $C = N_A p_{eff}^2 \mu_B^2/(3k_B T)$. Here, N_A is Avogadro's number, p_{eff} the effective magnetic moment, μ_B the Bohr magneton, and k_B the Boltzman constant. While C allows to determine the effective magnetic moment, i.e. $p_{eff}^2 = g^2 \cdot S(S+1)$ with the g-factor g the spin S, θ is a measure of the dominating magnetic interactions in the material. The fit shown in Fig. 6 yields the magnetic moment $p_{eff} = 0.5\ \mu_B$ and $\theta = -1$ K. The latter result implies negligible magnetic interactions between the paramagnetic moments. The small value of p_{eff} is consistent with ~10% of paramagnetic ions with $S = 1/2$ in the material, which agrees with 9% V^{4+}-ions ($S = 1/2$) present in the vanadyl groups. Note, that the small value of p_{eff} clearly shows that most of the ions are non-paramagnetic, i.e. the susceptibility data confirm Mo^{6+} and V^{5+} (both exhibiting $S = 0$) in the tunnel structure. Unlike other nanomaterials with mixed-valent V-ions such as VO_x-nanotubes, where the magnetic exchange can be very strong [15], the particular position of the magnetic V-sites inside the tunnel structure of $(VO)_{0.09}V_{0.18}Mo_{0.82}O_3 \cdot 0.54H_2O$ hinders significant magnetic exchange interactions as shown by the small value of θ.

In conclusion, we have presented a route to hydrothermally synthesize $(VO)_{0.09}V_{0.18}Mo_{0.82}O_3 \cdot 0.54H_2O$ using metallic Mo, $VOSO_4 \cdot nH_2O$, and H_2O_2 as the starting materials. The product adopts the hexagonal *h*-MoO_3 type structure with a rod-like morphology. It was found that the hexagonal MoO_3 structure can be stabilized at a higher temperature by the presence of VO^{2+} cations in the cavity of the framework. The material displays a paramagnetic response of essentially isolated spins presumably originating from the V^{4+}-ions in the vanadyl groups embedded in the tunnel structure. The observed paramagnetic moment confirms the expected number of magnetic V^{4+}-ions embedded in a matrix containing only non-magnetic Mo^{6+} and V^{5+} ions.

Acknowledgments

This work was supported by the Deutsche Forschungsgemeinschaft through grant KL 1824/2. R.K. acknowledges support by the BMBF via LIB 2015. Technical support by S. Pichl, M. Gierth, and G. Kreutzer is gratefully acknowledged.

References

[1] Song J, Ni X, Zhang D, Zheng H. Solid State Sci 2006;8:1164.
[2] Ramana CV, Atuchin VV, Troitskaia IB, Gromilov SA, Kostrosky VG, Saupe GB. Solid State Commun 2009;149:6.
[3] Dhage SR, Hassan MS, Yang OB. Mater Chem Phys 2009;114:511.
[4] Song J, Wang X, Ni X, Zheng H, Zhang Z, Ji M, et al. Mater Res Bull 2005;40:1751.
[5] Feist TP, Davies PK. Chem Mater 1991;3:1011.

[6] Hu Y, Davies PK, Feist TP. Solid State Ionics 1992;53–56:539.
[7] Mougin O, Dubois J-L, Mathieu F, Rousset A. J Solid State Chem 2000;152:353.
[8] Dupont L, Larcher D, Portemer F, Figlarz M. J Solid State Chem 1996;121:339.
[9] Hu Y, Davies PK. J Solid State Chem 1993;105:489.
[10] Olenkova IP, Plyasova LM, Kirik SD. React Kinet Catal Lett 1981;16:81.
[11] Dupont L, Larcher D, Touboul M. J Solid State Chem 1999;143:41.
[12] Zakharova GS, Täschner C, Volkov VL, Hellmann I, Klingeler R, Leonhardt A, et al. Solid State Sci 2007;9:1028.
[13] Song J, Ni X, Gao L, Zheng H. Mater Chem Phys 2007;102:245.
[14] Sotani N. Bull Chem Soc Jpn 1975;48:1820.
[15] Vavilova E, Hellmann I, Kataev V, Täschner C, Büchner B, Klingeler R. Phys Rev B 2006;73:144417.